

# Electromagnetic Scattering Using Physical Optics

Walton C. Gibson

Tripoint Industries, Inc.

tripoint@tripointindustries.com

December 1, 2005

## Abstract

This paper discusses the application of Physical Optics (PO) in three-dimensional frequency domain electromagnetic (EM) scattering and radiation problems where triangular subdomains (facets) are used to describe the scatterer. We first present the physical optics integral, and then derive a closed-form expression for this integral over an arbitrarily shaped triangle. We present the material in the context of incident plane wave scattering, however the methods used herein may be used for scattering as well as radiation problems.

## 1 The Electromagnetic Scattering Problem

When an electromagnetic (EM) wave  $\mathbf{E}^i$  is incident on an object, an electric surface current  $\mathbf{J}$  is induced on the object. These currents then radiate what is called the *scattered field*  $\mathbf{E}^s$ . Unfortunately for an arbitrarily shaped object, the induced currents cannot be solved for in closed form. A numerical technique such as the Method of Moments (MoM) [1] can be employed to solve the Electric Field Integral Equation (EFIE)

$$\mathbf{E}^s = -j\omega \frac{\mu}{4\pi} \iint_S \mathbf{J} \frac{e^{-jkR}}{R} ds - \nabla \frac{j}{4\pi\epsilon\omega} \iint_S \nabla \cdot \mathbf{J} \frac{e^{-jkR}}{R} ds \quad (1)$$

by enforcing the boundary conditions on electric field on the scatterer surface. The MoM generates a matrix equation which can be solved to obtain the currents due to an arbitrary excitation. The MoM is limited however by system memory and compute time, and often restricts an analysis to objects of small electrical size. For objects considered “large” compared to the wavelength, one can often make a decent approximation of the surface currents based on *a priori* knowledge of the EM physics. Physical Optics (PO) is one such approximation that works quite well in many cases.

## 2 Physical Optics For Conducting Objects

Consider an incident EM plane wave with  $\hat{\boldsymbol{\theta}}_i$  (vertical) and  $\hat{\boldsymbol{\phi}}_i$  (horizontal) components of electric field  $\mathbf{E}^i$  given by

$$\mathbf{E}^i = [E_{\theta}^i \hat{\boldsymbol{\theta}}_i + E_{\phi}^i \hat{\boldsymbol{\phi}}_i] e^{jk \hat{\mathbf{r}}_i \cdot \mathbf{r}} \quad (2)$$

and magnetic field  $\mathbf{H}^i$

$$\mathbf{H}^i = \frac{-\hat{\mathbf{r}}_i}{Z_o} \times \mathbf{E}^i = [E_{\phi}^i \hat{\boldsymbol{\theta}}_i - E_{\theta}^i \hat{\boldsymbol{\phi}}_i] \frac{e^{jk \hat{\mathbf{r}}_i \cdot \mathbf{r}}}{Z_o} \quad (3)$$

where  $\hat{\mathbf{r}}_i$  is a unit vector in the direction of incidence,  $\mathbf{r}$  a point on the scattering surface, and  $Z_o$  the impedance of free space  $Z_o = \sqrt{\frac{\mu_o}{\epsilon_o}}$ . For perfectly electrically conducting (PEC) objects, the surface current  $\mathbf{J}$  is derived from the magnetic field  $\mathbf{H}^i$  through the *physical optics equivalent*  $\mathbf{J} = 2\hat{\mathbf{n}} \times \mathbf{H}^i$ , where  $\mathbf{J}$  exists within the directly illuminated portion of the scatterer surface only [2]. This result is from image theory, where it is assumed that the surface is a perfectly flat, infinite electrical conductor. This expression for  $\mathbf{J}$  can be immediately inserted into (1) to obtain the scattered field, which in the far-zone requires only the first term, i.e.

$$\mathbf{E}^s = -j\omega \frac{\mu}{4\pi} \iint_S \mathbf{J} \frac{e^{-jk|\mathbf{r}_s - \mathbf{r}|}}{|\mathbf{r}_s - \mathbf{r}|} ds \quad (4)$$

where we have replaced  $R$  with  $|\mathbf{r}_s - \mathbf{r}|$ , the distance from the integration point  $\mathbf{r}$  to the observation point  $\mathbf{r}_s$  in the far-field. This integral is often simplified for far-zone observations by assuming that  $r_s \gg r$ . Therefore, we replace  $|\mathbf{r}_s - \mathbf{r}|$  in the denominator by  $r_s$  for amplitude variations, and by  $r_s - \hat{\mathbf{r}}_s \cdot \mathbf{r}$  in the exponential term for phase variations. Doing so, we write the above integral as

$$\mathbf{E}^s = -j\omega \frac{\mu}{4\pi} \frac{e^{-jk r_s}}{r_s} \iint_S \mathbf{J} e^{jk \hat{\mathbf{r}}_s \cdot \mathbf{r}} ds \quad (5)$$

Inserting the expression for the magnetic field  $\mathbf{H}^i$  from (3) into (5), we can write a final expression for the scattered field  $\mathbf{E}^s$  as

$$\mathbf{E}^s = -\frac{j}{\lambda} \frac{e^{-jk r_s}}{r_s} \hat{\mathbf{n}} \times (E_{\phi}^i \hat{\boldsymbol{\theta}}_i - E_{\theta}^i \hat{\boldsymbol{\phi}}_i) \iint_S e^{jk(\hat{\mathbf{r}}_s + \hat{\mathbf{r}}_i) \cdot \mathbf{r}} ds \quad (6)$$

The complete scattering response of an object can be specified by what is called the *scattering matrix*, which generates a set of co- and cross-polarized scattered fields. This matrix can be written as

$$\begin{bmatrix} E_{\theta}^s \\ E_{\phi}^s \end{bmatrix} = \begin{bmatrix} I_{\theta\theta} & I_{\theta\phi} \\ I_{\phi\theta} & I_{\phi\phi} \end{bmatrix} \begin{bmatrix} E_{\theta}^i \\ E_{\phi}^i \end{bmatrix} C \quad (7)$$

where we use the identity  $\mathbf{A} \cdot (\mathbf{B} \times \mathbf{C}) = \mathbf{B} \cdot (\mathbf{C} \times \mathbf{A})$  to write the following quantities

$$\begin{aligned} I_{\theta\theta} &= \hat{\mathbf{n}} \cdot (\hat{\boldsymbol{\theta}}_s \times \hat{\boldsymbol{\phi}}_i) \cdot I \\ I_{\phi\theta} &= \hat{\mathbf{n}} \cdot (\hat{\boldsymbol{\phi}}_s \times \hat{\boldsymbol{\phi}}_i) \cdot I \\ I_{\theta\phi} &= \hat{\mathbf{n}} \cdot (\hat{\boldsymbol{\theta}}_i \times \hat{\boldsymbol{\theta}}_s) \cdot I \\ I_{\phi\phi} &= \hat{\mathbf{n}} \cdot (\hat{\boldsymbol{\theta}}_i \times \hat{\boldsymbol{\phi}}_s) \cdot I \end{aligned} \quad (8)$$

and

$$I = \iint_S e^{jk(\hat{r}_s + \hat{r}_i) \cdot \mathbf{r}} d\mathbf{s} \quad C = -\frac{j}{\lambda} \frac{e^{-jk r_s}}{r_s} \quad (9)$$

The three-dimensional radar cross section (RCS) may be obtained from the incident and scattered electric field

$$\sigma = \lim_{r_s \rightarrow \infty} 4\pi r_s^2 \frac{|\mathbf{E}^s|^2}{|\mathbf{E}^i|^2} \quad (10)$$

where it is typically assumed that  $|\mathbf{E}^i| = 1$  for computational purposes.

### 2.0.1 Cross-Polarization

From the scattering matrix of Eqn. 8, it is obvious that in monostatic scattering, i.e. when  $\hat{r}_i$  and  $\hat{r}_s$  are the same,  $I_{\theta\theta} = I_{\phi\phi}$  and  $I_{\phi\theta} = I_{\theta\phi} = 0$ . In this case, the co-polarized fields are identical, and the cross-polarized fields are zero. The PO approximation does not involve non-uniform fringe currents, depolarizing scatterers, or multiple reflections. These effects come into play in with realistic, highly complex targets, and will be considered in subsequent papers.

## 3 The Physical Optics Integral

It is the integral  $I$  in Eqn. 9 on which we now focus our attention. To model a realistic scatterer surface for computer simulation, it is necessary to create a discretization that faithfully preserves its geometric shape, while still allowing a tractable and numerically efficient evaluation of the integral. One of the most popular methods of discretizations is a surface tessellation into a number of plane triangular patches (facets) [3]. Triangles have the advantage of being easy to generate, and they will conform quite well to a variety of surface curvatures. Such a tessellation is shown in Fig. 1 for a thin rectangular plate.

Let us assume we have discretized our surface  $S$  into a number of connected triangular patches, and let us further assume we have a method of computing which triangles are illuminated by the incident plane wave or shadowed. The PO integral  $I$  can now be written as a coherent summation of PO integrals over all illuminated triangles  $N_t$

$$I = \sum_{n=1}^{N_t} \iint_{T_n} e^{jk(\hat{r}_s + \hat{r}_i) \cdot \mathbf{r}} d\mathbf{s} \quad (11)$$

and our task now concerns finding a concise formula for  $I$  evaluated over each arbitrarily shaped plane triangle. From inspection, we see that this integral takes the form of a two-dimensional fourier transform over the triangle, the general form of which is

$$I = \iint_{T_n} f(x, y) e^{jk(ux + vy)} dx dy \quad (12)$$

This integral has received a great amount of attention in the literature, where analytic solutions for N-sided polygons have been derived by Gordon ([4], [5]) and Lee and Mittra [6].

Gordon employs the Green's theorem to convert the surface integral into a contour integral along the edges of the polygon. Lee and Mittra observe that since the boundary of the polygon is described by linear functions (its edges), the surface integral can be constructed by summing surface integrals at the polygon corners. Their result is

$$I = \sum_{n=1}^N e^{j\mathbf{w} \cdot \mathbf{r}_n} \left[ \frac{\hat{\mathbf{n}} \times \hat{\boldsymbol{\alpha}}_n \cdot \hat{\boldsymbol{\alpha}}_{n-1}}{(\mathbf{w} \cdot \hat{\boldsymbol{\alpha}}_n)(\mathbf{w} \cdot \hat{\boldsymbol{\alpha}}_{n-1})} \right] \quad (13)$$

where  $N$  is the number of polygon vertices,  $\hat{\mathbf{n}}$  is the polygon normal,  $\mathbf{w} = u\hat{\mathbf{x}} + v\hat{\mathbf{y}}$ ,  $\mathbf{r}_n$  is the  $n$ th polygon vertex, and  $\hat{\boldsymbol{\alpha}}_n$  are the normalized polygon edges

$$\hat{\boldsymbol{\alpha}}_n = \frac{\mathbf{r}_{n+1} - \mathbf{r}_n}{|\mathbf{r}_{n+1} - \mathbf{r}_n|} \quad (14)$$

with  $\mathbf{r}_0 = \mathbf{r}_N$ .

For the purposes of fast and efficient numerical calculation, it is highly desirable to obtain a more specialized solution for the integral over a triangle, which we will do in the next two sections using area coordinates. The result will be concise and convenient for software implementation.

### 3.1 Area Coordinates

In performing numerical integrations over triangular regions, it is often useful to make use of an orthogonal transformation to what are called *area coordinates* or *barycentric coordinates*. Analytic integrals are often easier to evaluate in area coordinates, and Gaussian quadrature tables are often presented in terms of them.

First let us consider a triangle  $T$  defined by the three vertices  $\mathbf{r}_1$ ,  $\mathbf{r}_2$  and  $\mathbf{r}_3$ . Any point  $\mathbf{r}$  located on the triangle may therefore be written as a weighted sum of these three vertexes, i.e.

$$\mathbf{r} = w\mathbf{r}_1 + u\mathbf{r}_2 + v\mathbf{r}_3 \quad (15)$$

where  $u$ ,  $v$  and  $w$  are variables called *area coordinates*. These are subject to the constraint

$$u + v + w = 1 \quad (16)$$

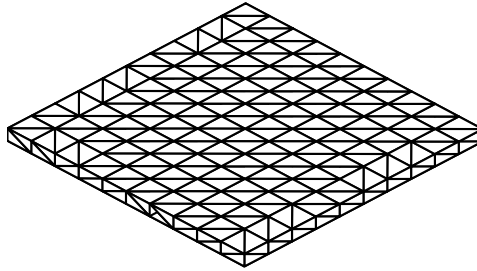


Figure 1: Rectangular Plate

which means that

$$w = 1 - u - v \quad (17)$$

hence

$$\mathbf{r} = \mathbf{r}_1 - u\mathbf{r}_1 - v\mathbf{r}_1 + u\mathbf{r}_2 + v\mathbf{r}_3 \quad (18)$$

Note that Eqn. 15 has the form of a linear interpolation. Indeed, area coordinates will also allow us to perform a linear interpolation at all points in a triangle if the values of the interpolated function is known at the vertices. The integral of a function  $f(\mathbf{r})$  on  $T$  can now be transformed to an integral in area coordinates as [1]

$$\int_T f(\mathbf{r}) ds = 2A \int_0^1 \int_0^{1-u} f((1-u-v)\mathbf{r}_1 + u\mathbf{r}_2 + v\mathbf{r}_3) dv du \quad (19)$$

where  $A$  is the area of the triangle. We will use Eqn. 19 to evaluate the PO integral  $I$  for a 3-sided polygon.

Given a point  $\mathbf{r}$  inside a triangle it is also often desirable to obtain the area coordinates  $u$ ,  $v$  and  $w$  at this point. We can write the barycentric expansion of  $\mathbf{r} = (x, y, z)$  in terms of the components of the triangle vertices as

$$\begin{aligned} x &= wx_1 + ux_2 + vx_3 \\ y &= wy_1 + uy_2 + vy_3 \\ z &= wz_1 + uz_2 + vz_3 \end{aligned} \quad (20)$$

substituting  $w = 1 - u - v$  into the above gives

$$\begin{aligned} x &= (1 - u - v)x_1 + ux_2 + vx_3 \\ y &= (1 - u - v)y_1 + uy_2 + vy_3 \\ z &= (1 - u - v)z_1 + uz_2 + vz_3 \end{aligned} \quad (21)$$

Rearranging, this is

$$\begin{aligned} u(x_2 - x_1) + v(x_3 - x_1) + x_1 - x &= 0 \\ u(y_2 - y_1) + v(y_3 - y_1) + y_1 - y &= 0 \\ u(z_2 - z_1) + v(z_3 - z_1) + z_1 - z &= 0 \end{aligned} \quad (22)$$

solving for  $u$  and  $v$  gives us

$$u = \frac{B(F + I) - C(E + H)}{A(E + H) - B(D + G)} \quad (23)$$

and

$$v = \frac{A(F + I) - C(D + G)}{B(D + G) - A(E + H)} \quad (24)$$

where

$$\begin{aligned}
A &= x_2 - x_1 \\
B &= x_3 - x_1 \\
C &= x_1 - x \\
D &= y_2 - y_1 \\
E &= y_3 - y_1 \\
F &= y_1 - y \\
G &= z_2 - z_1 \\
H &= z_3 - z_1 \\
I &= z_1 - z
\end{aligned} \tag{25}$$

### 3.2 PO Integral Evaluation

Transforming  $I$  from Eqn. 9 to area coordinates yields

$$2A \int_0^1 \int_0^{1-u} e^{jk(\hat{\mathbf{r}}_s + \hat{\mathbf{r}}_i) \cdot \mathbf{r}} dv du = 2A \int_0^1 \int_0^{1-u} e^{j\boldsymbol{\gamma}(u,v) \cdot \mathbf{r}(u,v)} dv du \tag{26}$$

where  $\boldsymbol{\gamma} = k(\hat{\mathbf{r}}_s + \hat{\mathbf{r}}_i)$ . Using Eqn. 18 for  $\mathbf{r}(u, v)$ , we can write the above as

$$\begin{aligned}
&2Ae^{j\boldsymbol{\gamma} \cdot \mathbf{r}_1} \int_0^1 \int_0^{1-u} e^{j\boldsymbol{\gamma} \cdot (\mathbf{r}_2 - \mathbf{r}_1)u} e^{j\boldsymbol{\gamma} \cdot (\mathbf{r}_3 - \mathbf{r}_1)v} dv du \\
&= 2Ae^{j\gamma_1} \int_0^1 e^{j\gamma_2 u} \int_0^{1-u} e^{j\gamma_3 v} dv du
\end{aligned}$$

where  $\gamma_1 = \boldsymbol{\gamma} \cdot \mathbf{r}_1$ ,  $\gamma_2 = \boldsymbol{\gamma} \cdot (\mathbf{r}_2 - \mathbf{r}_1)$ , and  $\gamma_3 = \boldsymbol{\gamma} \cdot (\mathbf{r}_3 - \mathbf{r}_1)$ .

Evaluating the integral over  $v$  gives yields

$$2Ae^{j\gamma_1} \int_0^1 e^{j\gamma_2 u} \left( \frac{e^{j\gamma_3 v}}{j\gamma_3} \Big|_0^{1-u} \right) du = 2Ae^{j\gamma_1} \int_0^1 e^{j\gamma_2 u} \left( \frac{e^{j\gamma_3(1-u)}}{j\gamma_3} - \frac{1}{j\gamma_3} \right) du$$

which can be rewritten

$$2A \frac{e^{j\gamma_1}}{j\gamma_3} \int_0^1 \left( e^{j\gamma_3} e^{ju(\gamma_2 - \gamma_3)} - e^{ju\gamma_2} \right) du$$

Integrating over  $u$  yields

$$\begin{aligned}
&2A \frac{e^{j\gamma_1}}{j\gamma_3} \left( \frac{e^{j\gamma_3} e^{j(\gamma_2 - \gamma_3)}}{j(\gamma_2 - \gamma_3)} - \frac{e^{j\gamma_2}}{j\gamma_2} \right) \Big|_0^1 \\
&= 2A \frac{e^{j\gamma_1}}{j\gamma_3} \left( \frac{e^{j\gamma_2}}{j(\gamma_2 - \gamma_3)} - \frac{e^{j\gamma_2}}{j\gamma_2} - \frac{e^{j\gamma_3}}{j(\gamma_2 - \gamma_3)} + \frac{1}{j\gamma_2} \right) \\
&= -2A \frac{e^{j\gamma_1}}{\gamma_3} \left( \frac{1 - e^{j\gamma_2}}{\gamma_2} + \frac{e^{j\gamma_2} - e^{j\gamma_3}}{\gamma_2 - \gamma_3} \right) \\
&= -2A \frac{e^{j\gamma_1}}{\gamma_3} \left( \frac{(\gamma_2 - \gamma_3)(1 - e^{j\gamma_2}) + \gamma_2(e^{j\gamma_2} - e^{j\gamma_3})}{\gamma_2(\gamma_2 - \gamma_3)} \right)
\end{aligned}$$

$$\begin{aligned}
&= -2A \frac{e^{j\gamma_1}}{\gamma_3} \left( \frac{\gamma_2 - \gamma_2 e^{j\gamma_2} - \gamma_3 + \gamma_3 e^{j\gamma_2} + \gamma_2 e^{j\gamma_2} - \gamma_2 e^{j\gamma_3}}{\gamma_2(\gamma_2 - \gamma_3)} \right) \\
&= -2A \frac{e^{j\gamma_1}}{\gamma_3} \left( \frac{\gamma_2 - \gamma_3 + \gamma_3 e^{j\gamma_2} - \gamma_2 e^{j\gamma_3}}{\gamma_2(\gamma_2 - \gamma_3)} \right) \\
&= -2A \frac{e^{j\gamma_1}}{\gamma_3} \left( \frac{1}{\gamma_2} + \frac{\gamma_3 e^{j\gamma_2} - \gamma_2 e^{j\gamma_3}}{\gamma_2(\gamma_2 - \gamma_3)} \right) \\
&= -2A \frac{e^{j\gamma_1}}{\gamma_2 \gamma_3} \left( 1 + \frac{\gamma_3 e^{j\gamma_2} - \gamma_2 e^{j\gamma_3}}{(\gamma_2 - \gamma_3)} \right) \\
&= -2A \frac{e^{j\gamma_1}}{\gamma_2 \gamma_3} \left( \frac{\gamma_2 - \gamma_3 + \gamma_3 e^{j\gamma_2} - \gamma_2 e^{j\gamma_3}}{(\gamma_2 - \gamma_3)} \right) \\
&= -2A \frac{e^{j\gamma_1}}{\gamma_2 \gamma_3} \left( \frac{\gamma_2(1 - e^{j\gamma_3}) - \gamma_3(1 - e^{j\gamma_2})}{(\gamma_2 - \gamma_3)} \right) \\
&= -\frac{2A e^{j\gamma_1}}{(\gamma_2 - \gamma_3)} \left( \frac{1 - e^{j\gamma_3}}{\gamma_3} - \frac{1 - e^{j\gamma_2}}{\gamma_2} \right)
\end{aligned}$$

Now, let us define the quantities  $\alpha_1 = \boldsymbol{\gamma} \cdot \mathbf{r}_1$ ,  $\alpha_2 = \boldsymbol{\gamma} \cdot \mathbf{r}_2$  and  $\alpha_3 = \boldsymbol{\gamma} \cdot \mathbf{r}_3$ . Hence,  $\gamma_1 = \alpha_1$ ,  $\gamma_2 = \alpha_2 - \alpha_1$  and  $\gamma_3 = \alpha_3 - \alpha_1$ . Making these substitutions into the above equation yields

$$= \frac{2A e^{j\alpha_1}}{(\alpha_2 - \alpha_3)} \left( \frac{1 - e^{j\alpha_2} e^{-j\alpha_1}}{\alpha_2 - \alpha_1} - \frac{1 - e^{j\alpha_3} e^{-j\alpha_1}}{\alpha_3 - \alpha_1} \right)$$

which yields the final result

$$I = \frac{2A}{(\alpha_3 - \alpha_2)} \left( \frac{e^{j\alpha_1} - e^{j\alpha_2}}{\alpha_1 - \alpha_2} - \frac{e^{j\alpha_1} - e^{j\alpha_3}}{\alpha_1 - \alpha_3} \right) \quad (27)$$

### 3.2.1 Special Cases

When  $\boldsymbol{\gamma}$  is perpendicular to any of the three edges, Eqn. 27 becomes singular, and a limiting case must be used. When  $\boldsymbol{\gamma} \cdot (\mathbf{r}_2 - \mathbf{r}_1) = \alpha_2 - \alpha_1 = 0$ , we take the limit

$$\lim_{(\alpha_2 - \alpha_1) \rightarrow 0} \frac{e^{j\alpha_1} - e^{j\alpha_2}}{\alpha_1 - \alpha_2} = j e^{j\alpha_1} \quad (28)$$

and use the formula

$$I = \frac{2A}{(\alpha_3 - \alpha_2)} \left( j e^{j\alpha_1} - \frac{e^{j\alpha_1} - e^{j\alpha_3}}{\alpha_1 - \alpha_3} \right) \quad \alpha_1 = \alpha_2 \quad (29)$$

likewise,

$$I = \frac{2A}{(\alpha_3 - \alpha_2)} \left( \frac{e^{j\alpha_1} - e^{j\alpha_2}}{\alpha_1 - \alpha_2} - j e^{j\alpha_1} \right) \quad \alpha_1 = \alpha_3 \quad (30)$$

and (some additional manipulations omitted)

$$I = \frac{2A}{(\alpha_1 - \alpha_2)} \left( j e^{j\alpha_3} - \frac{e^{j\alpha_1} - e^{j\alpha_3}}{\alpha_1 - \alpha_3} \right) \quad \alpha_2 = \alpha_3 \quad (31)$$

and when  $\gamma$  is normal to the facet (perpendicular to all three edges), we have the very simple case

$$I = Ae^{j\alpha_1} \tag{32}$$

## 4 Illumination and Shadowing

Previously, we assumed that we knew which triangles were illuminated by shadowed from the incident plane wave. For a single convex target such as a cube or sphere, the illumination can be determined by a dot product between each facet normal and the direction of incidence, assuming the normals are all outward facing. For a more complicated object that self shadow itself, or separate objects that shadow one another, computing the shadowing function for every triangle is more complicated. A common way of computing this information is to use a polygon ray tracer [7]. For each triangle, a line or *ray* is drawn from the center of that triangle in the direction of the incoming plane wave. If this ray passes through or intersects any other triangle on its way “out of the scene”, that triangle is said to be “blocked” or shadowed for that incident direction and the PO integral is not computed. This procedure is repeated for each triangle for every incident angle where the scattered field is to be calculated.

A triangle ray tracer relies on a ray-triangle intersection algorithm, which determines whether a ray intersects a triangle and if so, what the point of intersection is. There exist many schemes, such as the barycentric intersection algorithm by Moller and Trumbore [8]. The key to a good algorithm its is computational efficiency, as this routine will be called many times during the illumination calculation for each triangle. In the most naive scheme, the program would loop over all triangles in the model testing for an intersection with each ray. For models with many thousands of facets, this could impose a huge computational burden. Most practical ray tracers employ a heirarchical volume subdivision scheme such as a Binary Space Partition (BSP) [7] to

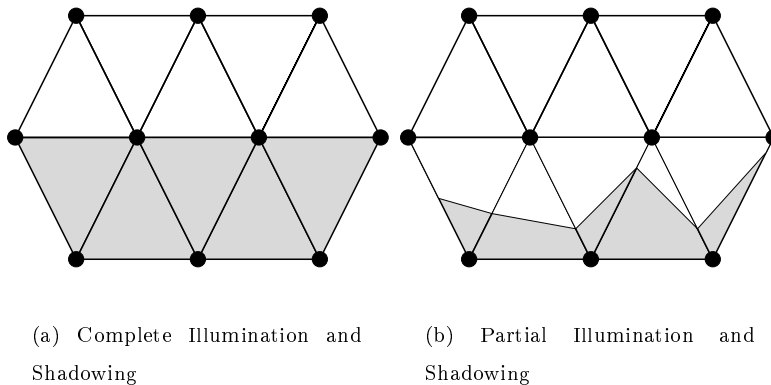


Figure 2: Illumination of Facet Geometry

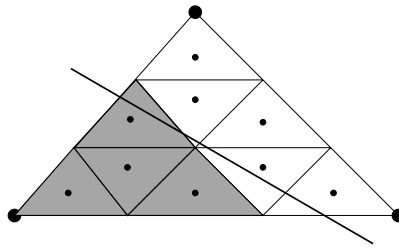


Figure 3: Facet Subdivision Into Sub Cells

reduce the number of intersection tests required for each ray.

## 4.1 Nonuniform Shadowing

We still must consider what happens if the surface of an individual facet is not uniformly illuminated. Fig. 2a illustrates a geometry where each facet is either totally illuminated or shadowed. Fig. 2b shows the same geometry where some of the facets are only partially illuminated. The configuration of Fig. 2b is what is encountered in realistic scattering problems.

Recall that Eqn. 27 was derived for a triangle that is completely illuminated. Therefore, we cannot use this expression for partially illuminated facets. What we can do is approximate this illumination by subdividing each facet into a number of sub-facets, each of which has the same geometric proportions as the “parent” facet. Retaining the shape allows us to reuse many of the geometric quantities across all sub-facets when we evaluate Eqn. 27. A continuous shadow line is shown drawn across a facet in Fig. 3. Sub-facets are said to be illuminated or shadowed if rays cast from each center is blocked. It is obvious from the figure that there will still be some amount of inaccuracy or “stair step” in this scheme, however if these sub-cells are made small enough, this inaccuracy can be minimized. The number of sub-cells should be based on the wavelength, such as requiring the maximum sub-cell edge length to be less than a predefined fraction of the wavelength (usually  $\frac{\lambda}{10}$  or less).

## 4.2 Z-Buffer Based Physical Optics

An alternative to the ray tracer or “facet-level” approach is Z-Buffer based PO. The Z-Buffer is a computer graphics algorithm often used for rendering complex scenes. In this method, triangles are transformed into screen space and drawn onto a virtual computer screen or “Z-Buffer”, which has the effect of computing the required illumination. This method was investigated by Rius et. al., who employed the graphics card in a computer workstation to perform the Z-Buffering operation [9]. In their scheme, the facet model of interest was rendered to the screen using the graphics library, and the final color and depth information read back out of the graphics buffer. The PO integral was approximated for a square pixel, and the backscattered field computed by

summing the contributions from each pixel using the information from the buffer.

In a later paper, Asvestas presents an alternative solution of the pixel-level PO integral with improved accuracy. The monostatic PO integral at the pixel level is

$$I = \iint_S e^{j2k\hat{\mathbf{r}}_i \cdot \mathbf{r}} (\hat{\mathbf{r}}_i \cdot \hat{\mathbf{n}}) ds \quad (33)$$

where  $\hat{\mathbf{r}}_i$  is the direction of incidence,  $\mathbf{r}$  is a point on the surface inside the pixel, and  $\hat{\mathbf{n}}$  is the surface normal inside the pixel. Asvestas notes that the depth  $z$  changes over the pixel surface, and uses a Taylor series expansion for the  $z$  in the  $\mathbf{r}$  term in Eqn. 33 to derive the following approximate result:

$$I \approx lh\eta_1(kl \frac{\hat{\mathbf{n}} \cdot \hat{\mathbf{x}}}{\hat{\mathbf{n}} \cdot \hat{\mathbf{z}}})\eta_1(kh \frac{\hat{\mathbf{n}} \cdot \hat{\mathbf{y}}}{\hat{\mathbf{n}} \cdot \hat{\mathbf{z}}})e^{2jz'} \quad (34)$$

where

$$\eta_1(x) = \sin(x)/x \quad (35)$$

and  $l$  and  $h$  are the width and height of each pixel, respectively,  $\hat{\mathbf{x}}$ ,  $\hat{\mathbf{y}}$ ,  $\hat{\mathbf{z}}$  are the local coordinate basis vectors for the screen, and  $z'$  is computed depth for the pixel.

Relying on the graphics subsystem of a workstation for rendering is undesirable for this process due to lower precision in the rendering hardware, latency and inefficiencies in the underlying graphics layer, a fixed resolution, and an overall lack of portability. A more general implementation of this method creates a virtual “computer screen” in system memory. For each incidence vector  $\hat{\mathbf{r}}_i$ , the virtual screen basis vectors in Fig. 4 are defined as

$$\begin{aligned} \hat{\mathbf{u}} &= \hat{\phi}^i \\ \hat{\mathbf{v}} &= -\hat{\theta}^i \end{aligned} \quad (36)$$

with  $\hat{\mathbf{z}} = \hat{\mathbf{u}} \times \hat{\mathbf{v}}$ . Assuming the object’s bounding box to have dimensions  $L_x$ ,  $L_y$ , and  $L_z$ , the screen must totally “enclose” the projection of the bounding box so that all portions of the object

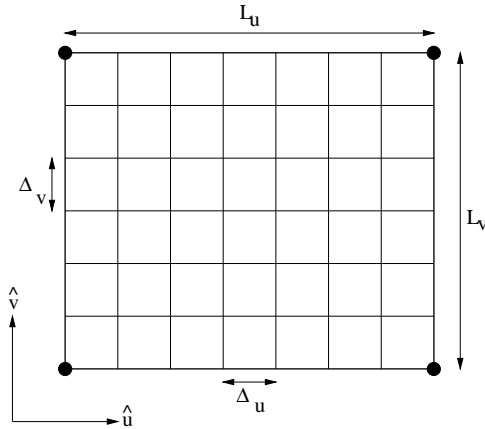


Figure 4: Z-Buffer Detail

will be rendered to the screen. The screen's dimensions  $L_u$  and  $L_v$  are

$$\begin{aligned} L_u &= |L_y \cos \phi^i| + |L_x \sin \phi^i| \\ L_v &= |L_x \cos \phi^i \cos \theta^i| + |L_y \sin \phi^i \cos \theta^i| + |L_z \sin \theta^i| \end{aligned} \tag{37}$$

The pixel width  $\Delta_u$  and height  $\Delta_v$  are chosen based on the operating wavelength. In practice, we have found that the pixel size should be less than or equal to about  $\frac{1}{50}$  of a wavelength for reasonable accuracy, as well as being small enough so that object features are sufficiently resolved in the buffer.

For each direction  $\hat{r}_i$ , a new screen with dimensions given by Eqn. 37 is created and each pixel's depth  $z$  is initialized to a very large negative value. Each triangle in the target model is put into the screen's local coordinate system by transforming each of its vertices. It is then "scan converted", in which the pixels on the screen covered by the triangle are filled. The depth for each pixel is interpolated between the  $z$  values of the triangle vertices as the triangle is rendered. Only if the depth is greater than the value currently in the pixel is the data in the pixel overwritten. After all facets have been processed, only those portions of the object which are closest to the screen remain in the Z-Buffer. The facets obscured by those closer to the screen are blocked from view.

For screens of very large size (2,000 or more pixels in each dimension), it may be necessary to break the screen into smaller pieces to work inside the available system memory. In this case, the above process would be repeated for each sub-screen with triangles clipped appropriately.

## References

- [1] S. Rao, D. Wilton, and A. Glisson, "Electromagnetic scattering by surfaces of arbitrary shape," IEEE Trans. Antennas Propagat., vol. 30, pp. 409-418, May 1982.
- [2] Balanis, Constantine. Advanced Engineering Electromagnetics. New York: John Wiley and Sons, 1989.
- [3] Foley, van Dam, Feiner and Hughes. Computer Graphics: Principles and Practice. Addison-Wesley, 1996.
- [4] W.B. Gordon, "Far-field approximations to the Kirchoff-Helmholtz representations of scattered fields," IEEE Trans. Antennas Propag., vol. 23, pp. 590-592, July 1975.
- [5] W.B. Gordon, "High frequency approximations to the physical optics scattering integral," IEEE Trans. Antennas Propag., vol. 42, pp. 427-432, March 1994.
- [6] S.W. Lee and R. Mittra. "Fourier transform of a polygonal shape function and its application in electromagnetics," IEEE Trans. Antennas Propagat., vol. 31, pp. 99-103, January 1983.

- [7] Glassner, Andrew S., Ed. An Introduction to Ray Tracing. Academic Press, 1989.
- [8] T. Moller and B. Trumbore, "Fast, Minimum Storage Ray-Triangle Intersection," *Journal of Graphics Tools*, 2(1):21-28, 1997
- [9] J. M. Rius, M. Ferrando, and L. Jofre, "High-frequency RCS of complex radar targets in real-time" *IEEE Trans. Antennas Propagat.*, vol. 41, pp. 1308-1311, Dec. 1993.
- [10] J. Asvestas, "The Physical-Optics Integral and Computer Graphics," *IEEE Trans. Antennas Propagat.*, vol. 42, pp. 1459-1460, Dec. 1995.